Effect of Molecular Weight and Branch Content on the Creep Behavior of Oriented Polyethylene

P. A. O'Connell,* M. J. Bonner, R. A. Duckett, I. M. Ward

IRC in Polymer Science and Technology, Department of Physics and Astronomy, University of Leeds, Leeds LS2 9JT, United Kingdom

ABSTRACT: Creep studies were carried out on a range of homopolymers and copolymers of polyethylene with well-defined molecular weight and branch content. The creep data were analyzed in terms of two thermally activated processes acting in parallel and the effects of molecular weight and branch content are discussed. It is shown that increasing either the number-average molecular weight or the weight-average molecular weight gives improved creep behavior at all stress levels. The introduction of butyl branches leads to lower creep at low-stress levels but can give rise to higher creep at high stress. Plots of the equilibrium $\log_{10}$(strain rate) versus stress at fixed draw ratio (strain) can be used to define sections through a unique true stress/true strain/strain rate surface for each material. These creep results have an additional value in terms of the link between slow crack propagation (SCG) in polyethylene and fibril creep, confirming the proposal made elsewhere that SCG can be quantified in terms of creep to failure across the true stress/true strain/strain rate surface. © 2003 Wiley Periodicals, Inc. J Appl Polym Sci 89: 1663–1670, 2003

Key words: creep; polyethylene (PE); molecular weight distribution; stress; strain

INTRODUCTION

The presence of a flaw or crack in a bulk material leads to a stress concentration at the crack tip that, to prevent the formation of a stress singularity, produces a yield zone. Within the yield zone there are small voided regions and as the crack grows these regions grow and join to form a craze. The structure of such a craze is complicated but essentially consists of filaments of oriented material (fibrils) bridging the boundaries of the crack.

Work by Bhattacharya and Brown[1] has identified the processes involved in the growth of such a craze. At the craze tip, material is continually yielding to form new voided material that, in turn, creates new fibrillar material. At the tip of the crack, the craze fibrils grow by drawing in of new material at the bulk/fibril interface and the subsequent creep of this oriented material. The craze increases in length and thickness approximately linearly with time until fibril failure occurs, after which rapid crack growth can occur, leading to ultimate bulk section failure. Importantly, the time for fibril failure to occur can be a significant proportion of the total failure time and it seems likely that the formation and deformation of the fibrils are a major factor in the lifetime of such materials.

Data have been reported[2] that show a strong link between the stress crack resistance of polyethylene and its creep behavior. The idea has also been developed by the present authors[3] to identify quantitative relationships between slow crack propagation and long-term creep of oriented polyethylenes. The key conceptual step in the latter study was to consider that the material in the craze deforms similarly to an oriented (drawn) monofilament as it gradually extends from its initial (so-called natural) draw ratio as it enters the craze, until failure occurs. Central to the quantification of this idea is that there exists a true stress/true strain/strain rate surface, such that the relationship between stress and strain rate can be defined for any strain (i.e., draw ratio); thus the time taken for an element in the craze to cross this surface and extend to failure is uniquely determined.

These considerations suggest that there is considerable merit in extending previous studies of the creep behavior of oriented polyethylenes that were originally undertaken to define the limits of performance of oriented polyethylenes, either as high-modulus fibers or as geo-textile grids. In particular, previous studies were limited to samples of fixed (final) draw ratio, not samples that are continuously drawing, as is envisaged in a craze. The early creep studies clearly identified the improvements in creep performance achieved by increasing molecular weight and/or

---

Correspondence to: I. M. Ward (I.M.Ward@leeds.ac.uk).

**Present address:* Department of Chemical Engineering, Texas Tech University, Box 43103, Lubbock, TX 79409-3103.

TABLE I
Characteristics of Polymers Studied

Polymer	M_w ($\times 10^{-3}$)	M_n ($\times 10^{-3}$)	Butyl/1000 C branches
PE1	134	18	0
PE2	200	30	0.5
PE3	350	28	0
PE4	200	75	0
PE5	200	18	0
PE6	150	18	0.5
PE7	200	18	5.7

short-chain branching. It was later evident that slow crack performance follows an analogous pattern of behavior. In this study, we explore in particular the effects of number-average (M_n) and weight-average (M_w) molecular weight. In addition, three copolymers were studied to assess the effect of branch content.

EXPERIMENTAL

Materials

A range of polyethylene homopolymers with well-defined molecular weights was studied (Table I). Materials PE1, PE3, PE4, and PE5 are homopolymers chosen to identify the respective influence of M_n and M_w. PE2, PE6, and PE7 are copolymers with known concentrations of butyl branches.

Sample preparation

All polymers were compression molded between polished brass plates for 5 min at 160°C and then slow cooled at a controlled rate of 2°C/min. Typical sheet

thickness was 0.3 mm. Dumbbell-shape samples (gauge length, 18 mm; width, 5 mm) were cut from the sheet and dots placed at 2-mm intervals along the center line of the gauge section. The samples were then drawn at room temperature in an Instron 4505 tensile testing machine at a crosshead speed of 10 mm/min to their natural draw ratio λ_n. All samples showed a distinct yield point (indicated by a peak in the load–displacement curve) and subsequent formation of a neck region in the gauge length containing oriented material. Figure 1 is a schematic diagram showing the whole of the deformation behavior in terms of nominal stress against strain.

To prepare a creep sample the crosshead was run until the sample had reached the required draw ratio (generally the natural draw ratio when the neck reaches the shoulders of the dumbbell). The drawn sample was then removed and allowed to relax at room temperature for 24 h. A suitable length (between 70 and 100 mm) was then cut from the drawn region of the sample for further testing.

Mechanical tests

Creep tests were carried out on dead-loading creep rigs designed and built within the Department of Physics as described in detail elsewhere.[5] In brief, these creep rigs consisted of a fixed upper clamp to which one end of the sample was attached (Fig. 2). The lower end was attached to a weight holder, which in turn was attached to the core of a linear voltage displacement transducer. The coil of the transducer was mounted in a holder that could move vertically in discrete steps of 20 mm. This setup had the dual advantage of both accommodating samples of differ-
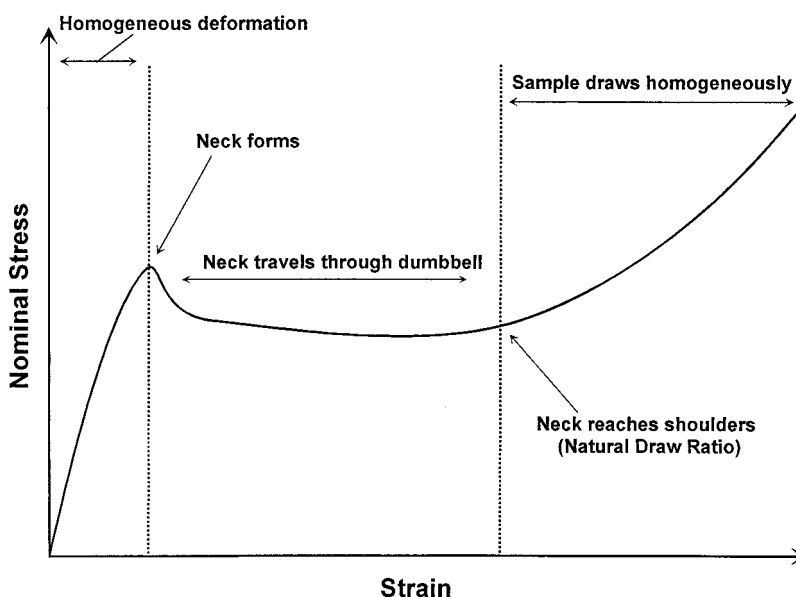

Figure 1 Typical stress–strain curve for drawing of PE showing different regions of the drawing.
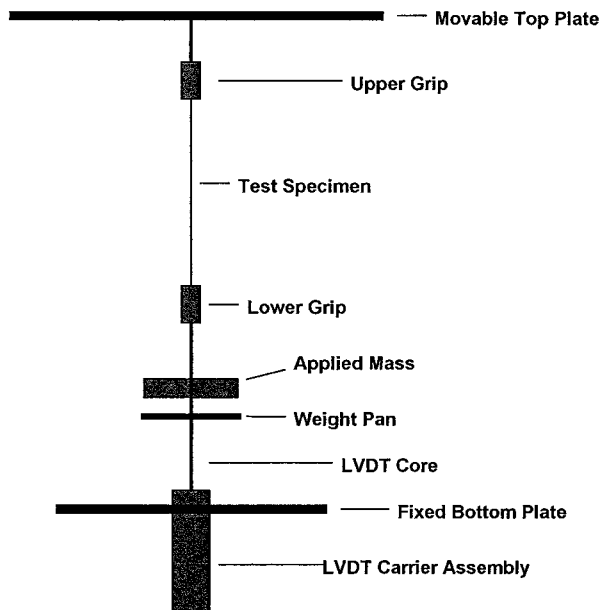
Figure 2 Schematic diagram of creep apparatus.

ing gauge length and allowing for continued measurements when the creep extension exceeded the calibrated range of the transducer. The output from the transducers was monitored by a computer, using a program that automatically recorded the time at which each increment in a nominal strain of 0.2% occurred. A typical gauge length for the creep tests was 60 mm, with the actual length measured to 0.2 mm.

The creep rigs were housed in a temperature-controlled laboratory, where the temperature was maintained at 20°C to within 2°C. In addition, each rig was equipped with an environmental chamber, thus allowing testing to be carried out at elevated temperatures. Heating was achieved by passing compressed air over a heating coil before it entered the chamber. The temperature was controlled to within 0.5°C using a Eurotherm 808 with the thermocouple at the center of the heating chamber.

Tensile tests on the oriented material were carried out on an Instron 4505 machine. Drawn material was cut to 80-mm lengths and 15 mm of each end was masked off with tape, leaving a 50-mm gauge length. The tape on each end provided sufficient cushioning so that the samples were not damaged when being loaded in the clamps. The crosshead was driven under computer control at a fixed speed and the load and displacement were recorded on the computer at predefined time intervals.

Data analysis

Data from the creep test were in the form of time, strain on the sample (ϵ), and strain rate ($\dot{\epsilon}$). If the

original sample cross-sectional area (XS) and natural draw ratio λ_n are known, then the initial true stress (σ_N) can be calculated for a given load (L).

At any given time the current true stress (σ_T) and true draw ratio (λ_T) can be calculated, as follows:

$$\sigma_T = (1 + \varepsilon)\sigma_N$$

$$\lambda_T = (1 + \varepsilon)\lambda_N$$

where ϵ is the engineering creep strain measured from the drawn state.

Data from the Instron tests were in the form of extension versus load and these were used in a similar way to calculate the true draw ratio (λ_T), true stress (σ_T), and true strain rate ($\dot{\epsilon}$) (all referred back to the isotropic state).

Data from each test thus allowed the calculation of true stress/true strain/strain rate throughout the duration of the test. Using a wide range of initial starting conditions, a three-dimensional surface can be mapped out in detail. It is important to note here that, although both types of experiments would result in a stress/strain/strain rate surface, they were mapped out using different paths over that surface. In the case of creep, the stress and strain were effectively imposed and the resulting strain rate was measured. For the Instron tests, the strain rate and strain were imposed and the resulting load or stress was measured. A unique surface exists if any combination of two of the three variables determines the third, irrespective of which path is used to reach that point.

RESULTS AND DISCUSSION

Creep

The creep data were analyzed as mentioned above and are presented in the form of Sherby–Dorn plots,[6] that is, as $\log_{10}$(strain rate) versus strain at a nominal stress level. Figures 3 and 4 show the results for homopolymers PE3 and PE5, respectively; the stress levels given are the true stresses when the material is at a draw ratio of 10. Figure 3 shows the typical characteristics of this type of plot. On loading, at low strains, there is an initial steep region where the strain rate drops rapidly with strain. The material then enters a second stable region, where the strain rate dependency on strain is considerably less.

The first, steep region is explained as a combination of two factors: (1) the "instantaneous" linear elastic response of the material to the application of the load and (2) a memory effect, where the material remembers it went to a higher strain on the initial drawing, before being allowed to relax for 24 h before testing. As such this first region does not reflect a true creep response of the material and is generally disregarded
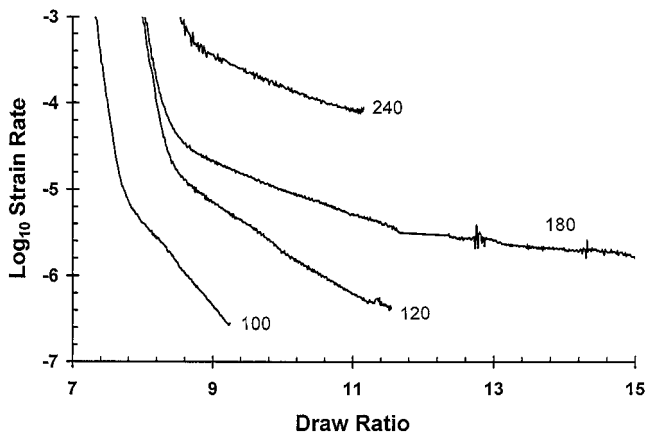
Figure 3 Sherby–Dorn plots for the PE3 material. Stress levels in MPa at a draw ratio of 9.

Figure 5 Plot of $\log_{10}$(strain rate) versus true stress for the PE5 material at a draw ratio of 9 under creep ($\triangle$) and constant crosshead (■) conditions.

(removed from Fig. 4 for clarity). In the second region the strain rate dependency on strain can continue to decrease with increasing strain until the creep strain rate stabilizes and becomes constant. For highly drawn samples such "plateau" creep rates are quite frequently observed and have been the subject of detailed interpretation[7] (Fig. 3). Alternatively, the material response may be such that the $\log_{10}$(strain rate) will decrease essentially linearly with increasing strain (Fig. 4). Both figures also show that at very low stress levels the slope of decreasing strain rate with increasing strain can be very steep, suggesting extremely slow creep rates at modest strains and low stresses.

Instron tests

Tensile tests at a constant crosshead speed were conducted on drawn samples of each material. As shown above, from a knowledge of the original sample dimensions and the initial draw ratio, it is possible at each point in the test to calculate the true stress, strain, and strain rate that the sample is experiencing.
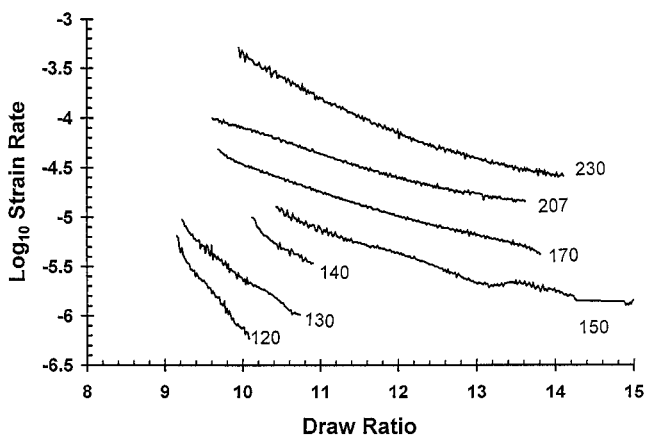

Figure 4 Sherby–Dorn plots for the PE5 material. Stress levels in MPa at a draw ratio of 9.
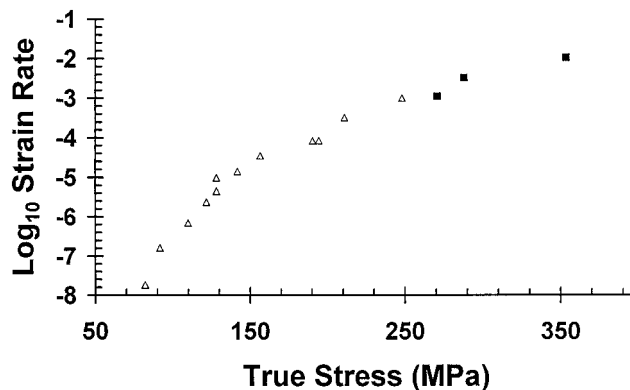
Analysis

The creep response of the different materials was compared by looking at the $\log_{10}$(strain rate) as a function of true stress at a fixed strain, in essence taking a slice through each stress/strain/strain rate surface at a given draw ratio. The choice of draw ratio was limited by having to be higher than the largest natural draw ratio but lower than the minimum failure draw ratio, and a draw ratio of 9 was found to be the best compromise for the homopolymers and lightly branched copolymers (PE2 and PE6). The maximum usable draw ratio for PE7 copolymer was comparable to the natural draw ratio of the PE5 copolymer and so, for this material only, the data were analyzed at a draw ratio of 7.

The first step in the analysis was to compare the data from the creep tests and the Instron tests to confirm that we were looking at a unique surface. Previous work on a range of polyethylenes showed this to be the case in both the isotropic and oriented state.[8–10] Figure 5 shows the data set for the PE5 material. As can be seen, the agreement is excellent and although not shown, similar agreement is found for all the materials in this study. (For detailed studies of PE6 and PE7, see Bonner.[10]) This is further confirmation that the stress/strain/strain rate surface is unique and that access to any point on the surface is path independent.

Room-temperature creep

Effect of number-average molecular weight

The effect of number-average molecular weight (M_n) is shown in Figure 6(a) and (b), where the $\log_{10}$(strain rate) versus true stress data at a draw ratio of 9 are plotted for materials of different M_n and similar or nearly identical M_w. The comparison between PE4 and PE5 in Figure 6(a) is particularly revealing, in that these polymers both have M_w values close to 200,000.
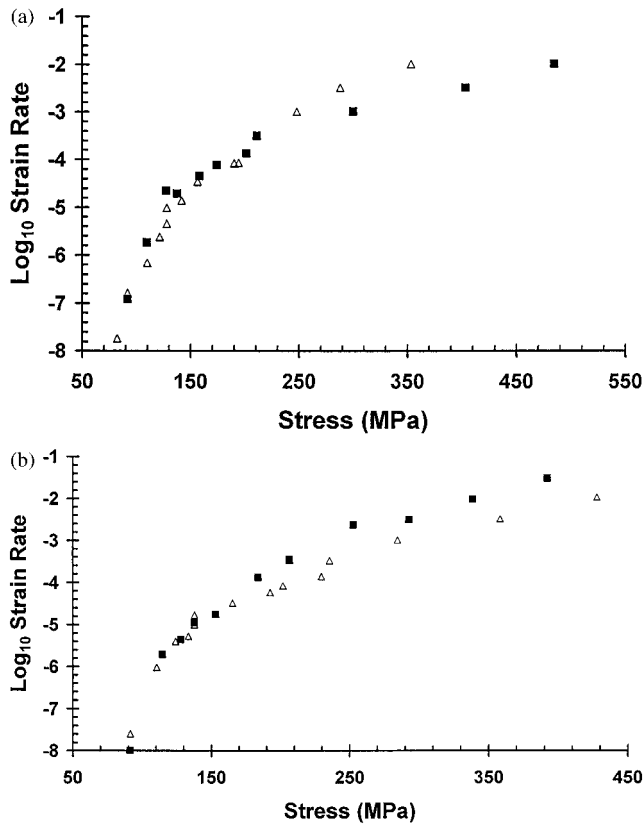
Figure 6 Effect of M_n on the $\log_{10}$(strain rate) versus true stress creep response at a draw ratio of 9: (a) homopolymers PE5 ($\triangle$) and PE4 ($\blacksquare$) at constant M_w; (b) copolymers PE2 ($\triangle$) and PE6 ($\blacksquare$) at constant branch content and similar M_w.

Figure 6(b) shows the creep behavior of PE2 and PE6, polymers of similar low branch content (0.5 branches/1000 carbon atoms) and fairly close M_w (150–200,000). In both these comparisons there is a low-stress region where the strain rate is highly stress dependent, with a transition region between these two extremes. Data in the low-stress region are difficult to obtain, primarily because of the very long experimental times needed at these low rates. The low-stress region will be considered later; for now we will concentrate on the transition and high-stress regions.

The curves for each material merge in the transition region, with no clear molecular weight effect. However, the high-stress region shows a very clear trend with respect to molecular weight, whereby the strain rate dependency on stress increases with decreasing M_n. Because the data merge in the transition region, this leads to a "fanning out" of the data at increasing stress levels. Therefore, for a given stress in the higher stress region, the creep rate decreases for materials of increasing M_n.

A model originally proposed by Wilding and Ward[7,11,12] has been successfully used to describe this type of process. It proposes that the system can be modeled as two activated processes acting in parallel;

that is, both processes produce the same strain rate and the sum of the stresses on the two processes is equal to the applied stress σ. This is described mathematically by the following equations:

$$\dot{\varepsilon} = \dot{\varepsilon}_{01}\exp\left(\frac{\Delta U_1}{kT}\right)\sinh\left(\frac{\sigma_1 v_1}{kT}\right) = \dot{\varepsilon}_{02}\exp\left(\frac{\Delta U_2}{kT}\right)\sinh\left(\frac{\sigma_2 v_2}{kT}\right) \tag{1}$$

and $\sigma = \sigma_1 + \sigma_2$, where $\dot{\varepsilon}_{0i}$, ΔU_i, and v_i are the preexponential, activation energy, and activation volume, respectively, for the two processes, $i = 1$ and 2; k is the Boltzmann constant; and T is the absolute temperature.

In the "low" strain rate region (still relatively high for process 1) the stress carried by process 2 is negligible and the system can be described by

$$\log(\dot{\varepsilon}) = \log\left(\frac{\dot{\varepsilon}_{01}}{2}\right) - \left(\frac{\Delta U_1}{kT}\right) + \left(\frac{\sigma v_1}{2.3kT}\right) \tag{2}$$

For high strain rates both processes are active and the system can be represented by the following:

$$\log(\dot{\varepsilon}) = \left(\frac{v_1 v_2}{v_1 + v_2}\right)\left[\frac{\log(\dot{\varepsilon}_{01})}{v_1} + \frac{\log(\dot{\varepsilon}_{02})}{v_2}\right]$$
$$- \left(\frac{\Delta U_1}{v_1} + \frac{\Delta U_2}{v_2}\right) + \frac{\sigma v_1 v_2}{2.3kT(v_1 + v_2)}$$

It is clear that in both low and high strain rate regimes there is an approximately linear dependency of $\log(\dot{\varepsilon})$ on stress, as observed experimentally, with a gradient of $v_e/2.3kT$. Furthermore, in the high strain rate region there is an effective activation volume

$$v_e = \frac{v_1 v_2}{v_1 + v_2}$$

and effective activation energy ΔU_e such that

$$\frac{\Delta U_e}{v_e} = \frac{\Delta U_1}{v_1} + \frac{\Delta U_2}{v_2}$$

A least-squares fit to the high stress data of Figure 6(a) and (b) gives effective activation volumes $[(v_1 v_2)/(v_1 + v_2)]$ of $v_e = 88 \pm 8$ Å^3 (PE5), 86 ± 4 Å^3 (PE6), 66 ± 4 Å^3 (PE2), and 50 ± 4 Å^3 (PE4).

Increasing the M_n is therefore reflected in terms of the two-process model as a reduction in the activation volume of the high-stress process. However, it must be recognized that the data from the PE5 corresponded to a draw ratio of 7, compared to the other materials at $\lambda = 9$.
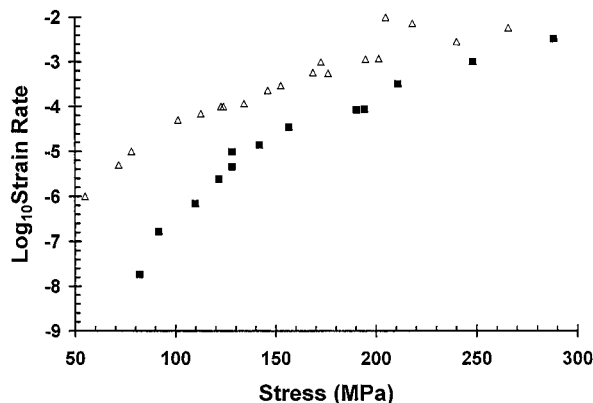
Figure 7 Effect of M_w on the $\log_{10}$(strain rate) versus true stress creep response at a draw ratio of 9 (PE1, △; PE5, ■).

Effect of weight-average molecular weight

The effect of M_w is most clearly shown by the comparison in Figure 7 of the creep behavior of the homopolymers PEl and PE5, both of which have M_n values of 18,000 but different M_w values. In this case, there is a major effect over the whole stress range, with the higher molecular weight polymer showing greatly reduced creep rates despite having a lower draw ratio. This is entirely consistent with previous creep measurements by Ward and Wilding[7] and the corresponding improvements in slow crack propagation reported by Clutton et al.[13]

Effect of copolymer content

The effect of branch content on creep behavior is shown in three comparisons, represented in Figure 8(a), (b), and (c). The comparisons of Figure 8(a) and (b), including PE7, which has 5.7 branches/1000 C atoms, are clearest and the strain rate/stress curves cross those for no branch content (PE5) or 0.5 branches/1000 C atoms (PE2). It appears that the low-stress process is significantly reduced in magnitude by high branch content, consistent with significant reductions in slow crack growth observed by several investigators.[13,14] The high-stress process, on the other hand, shows higher creep, consistent with the reduction of the yield stress with increasing branch content, which has conventionally been attributed to a significant reduction in crystallinity.

The comparison of the creep behavior of PE1 and PE6 shown in Figure 8(c) shows the interesting combined effect of increasing M_w at constant M_n, together with simultaneously introducing a comparatively small number of branches (0.5/1000 C atoms). There is a significant reduction in the creep at every stress level. These results are consistent with the sensitivity of slow crack growth to similar changes in M_w and branch content.[13]

Elevated temperature creep

Referring back to Figure 6, it is apparent that at stresses ≤ 100 MPa, the strain rate decreases rapidly. As a consequence, the timescale required to collect these data rapidly extends to many months/year. We mentioned previously that the $\log_{10}$(strain rate) : stress response can be modeled as two Eyring activated processes acting in parallel and that in the high- and low-stress regions the relevant process can be approximated to a single dominant activated process. For a single Eyring process, eq. (2) can be written as
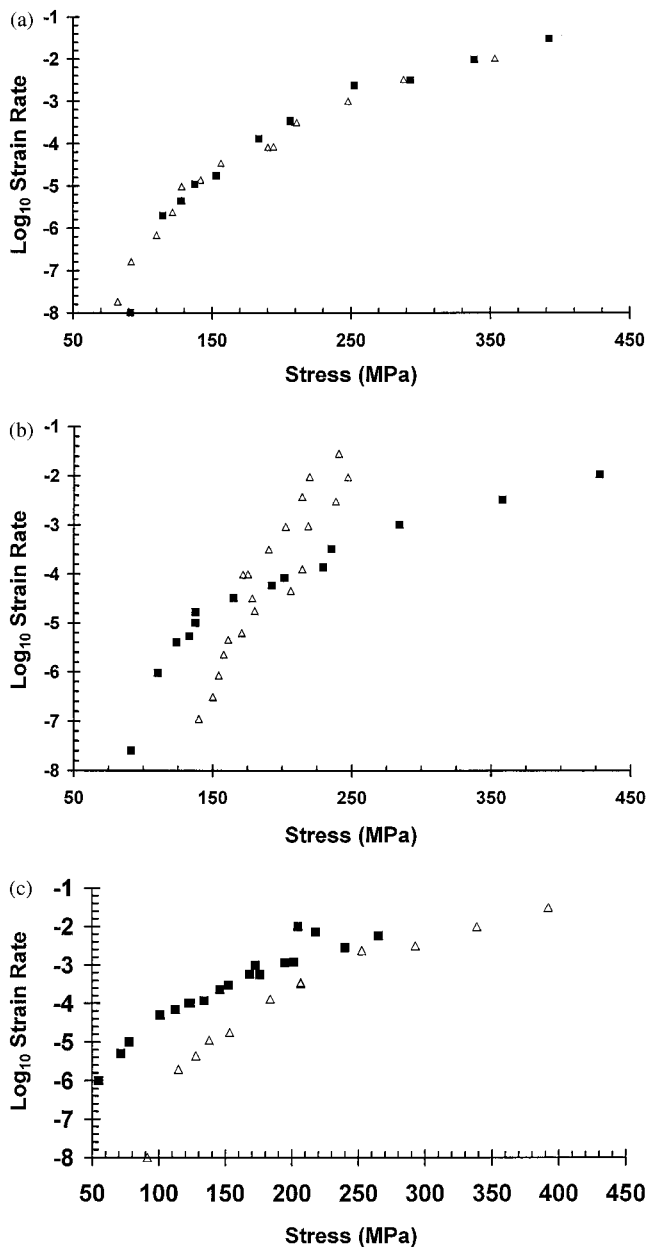

Figure 8 Effect of copolymer content on the $\log_{10}$(strain rate) versus true stress creep response: (a) comparison of PE5 (△) and PE6 (■) at a draw ratio of 9; (b) comparison of PE7 (△) at a draw ratio of 7 and PE2 (■) at a draw ratio of 9; (c) comparison of PE6 (△) and PE1 (■) at a draw ratio of 9.
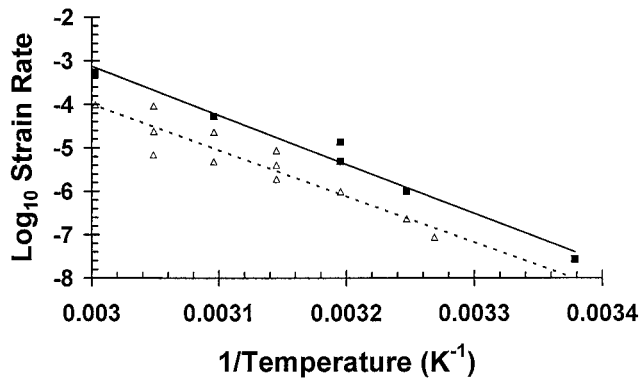
Figure 9 Plot of $\log_{10}$(strain rate) versus reciprocal temperature for the PE2 material at stress levels of 90 MPa ($\triangle$) and 100 MPa ($\blacksquare$) at a draw ratio of 9.

$$\log(\dot{\varepsilon}) = \log(\dot{\varepsilon}/2) - (\Delta U_e - \sigma v_e)/2.3kT \qquad (3)$$

where the symbols are as described earlier. This suggests we can use elevated temperatures to shift the low-stress process to shorter timescales (i.e., higher rates).

Elevated temperature creep tests were conducted on four polymers, PE2, PE3, PE4, and PE5, over a range of temperatures from 23 to 70°C at stresses of 90 and 100 MPa (as measured at a draw ratio of 9). Figures 9–12 show the data plotted as $\log_{10}$(strain rate) versus $1/T$. As is common with creep data there is some degree of scatter, although the data are essentially linear in nature.

Linear regression was applied to the data, allowing the $\log_{10}$(strain rate) to be determined at 23°C at both 90 and 100 MPa. By rearranging eq. (2) we have

$$v_e = 2.3kT\{d(\log[\dot{\varepsilon}]/d(\sigma)\}$$

Hence, the strain rates determined above for the stress change from 90 to 100 MPa can be used to determine the activation volumes in this low-stress regime. Furthermore, from eq. (3) a plot of $\log(\dot{\varepsilon})$ versus $1/T$ yields a straight line of gradient
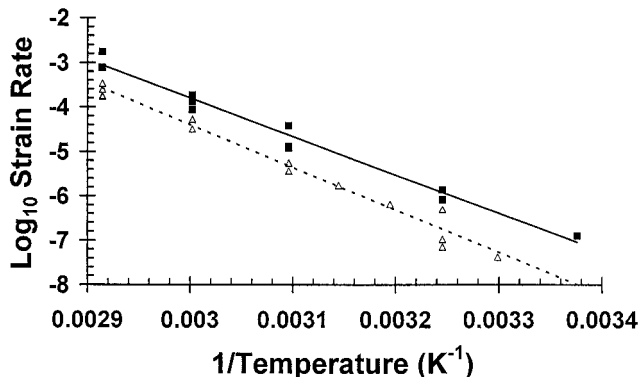

Figure 10 Plot of $\log_{10}$(strain rate) versus reciprocal temperature for the PE3 material at stress levels of 90 MPa ($\triangle$) and 100 MPa ($\blacksquare$) at a draw ratio of 9.
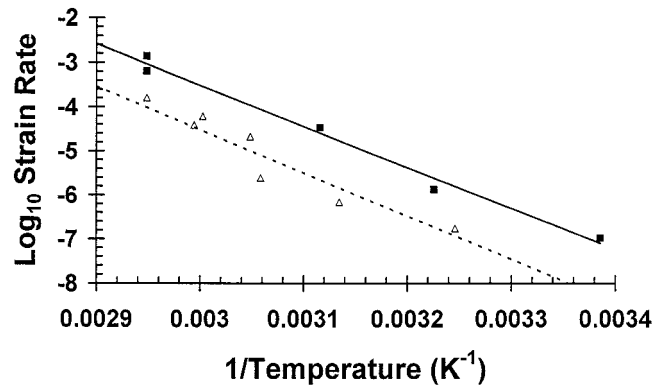

Figure 11 Plot of $\log_{10}$(strain rate) versus reciprocal temperature for the PE4 material at stress levels of 90 MPa ($\triangle$) and 100 MPa ($\blacksquare$) at a draw ratio of 9.

$$\Delta U_e - \sigma v_e/2.3k$$

Thus, if one knows the activation volume (v_e), the activation energy (dU) can then be calculated. The values derived from this approach are listed in Table II. Note that, in view of the scatter apparent in the data, the estimated errors are quite large ($\sim$ 15%), although general trends can be determined.

There is a clear trend in that the activation volume increases with increasing M_n and M_w. There is no clear trend in activation energies, although the value for the low M_n material PE5 is noticeably smaller than that of the others; however, with the associated errors no significant differences can be determined (PE5 also has the lowest draw ratio).

The trend in activation volume with molecular weight is particularly interesting because it is the reverse of that seen with the same materials in the high-stress regime, where the activation volume decreased with increasing M_w or M_n. Bearing in mind that all the data tend to merge at the transition point, then in the high-stress region the PE5 material, by virtue of having a higher activation volume, always
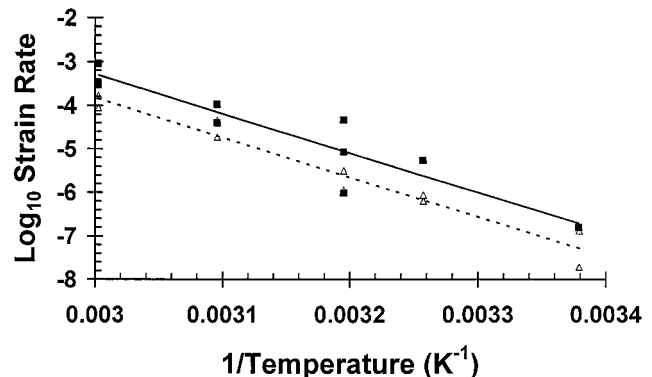

Figure 12 Plot of $\log_{10}$(strain rate) versus reciprocal temperature for the PE5 material at stress levels of 90 MPa ($\triangle$) and 100 MPa ($\blacksquare$) at a draw ratio of 9.

TABLE II
Analysis of High-Temperature Creep Data

Polymer	Activation volume (Å^3)	Activation energy (kcal/mol)	M_n	M_w	Branch content
Samples with increasing M_n					
PE5	558 (110)	49 (7)	18	200	0
PE2	697 (140)	59 (9)	30	200	0.5
PE4	1058 (210)	59 (9)	75	200	0
Samples with increasing M_w					
PE2	697 (140)	59 (9)	30	200	0.5
PE3	863 (170)	54 (8)	28	350	0

exhibits a higher creep rate than that of the PE2 and PE4 materials at a given stress. Conversely, in the low-stress regime, despite having a lower activation volume, it still exhibits a higher creep rate at a given stress (Fig. 13). It is possible that the creep rate for the low molecular weight polymer is always greater than or equal to the rate for the higher molecular weight polymer, at any given stress, because of differences in preexponential factors, $\dot{\varepsilon}_{01}$ and $\dot{\varepsilon}_{02}$ for the different molecular weights.

CONCLUSIONS

All the homopolymers show a transition regime from process 1 to process 2 at approximately the same stress : strain rate values. In the high-stress regime, the activation volume increases with decreasing molecular weight (both M_n and M_w). Thus, samples of lower molecular weight have a higher creep rate at a given stress level. Conversely, in the low-stress regime, the activation volume decreases with decreasing molecular weight (both M_n and M_w). However, because the transition region is the same for all the homopolymers, then samples of lower molecular weight will again have a higher creep rate at a given stress level. In general, therefore, samples with increasing molecular

weight (both M_n and M_w) have improved creep performance at all stress levels.

The incorporation of 4.5 butyls per 1000 carbon atoms has a dramatic influence on the creep behavior, increasing the high stress activation volume fourfold and shifting the transition region to a lower rate/higher stress. The result is a significantly improved creep performance over the majority of the stress range. These creep results, together with the proven existence of a true stress/true strain/strain rate surface for a given material, confirm the origin of the known effects of molecular weight and copolymer content on the slow crack growth behavior of polyethylene, that is, the importance of creep to failure in the oriented fibrils within the craze.[3,15]
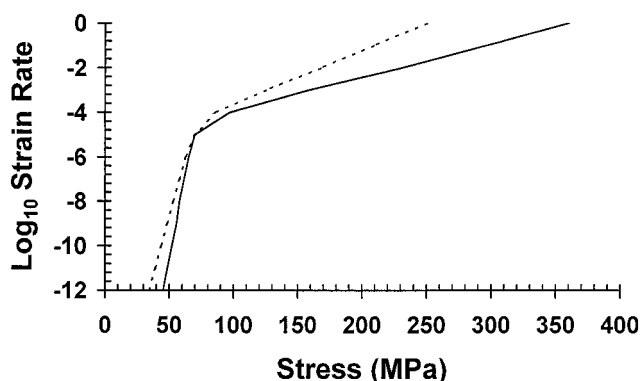
Figure 13 Two-process model showing the effect of changes in activation volume on the overall creep response (solid line, high molecular weight; dashed line, low molecular weight).

References

1. Bhattacharya, S. K.; Brown, N. J Mater Sci 1984, 19, 2519.
2. Cawood, M. J.; Channell, A. D.; Capaccio, G. Polymer 1993, 34, 423.
3. O'Connell, P. A.; Bonner, M. J.; Duckett, R. A.; Ward, I. M. Polymer 1995, 36, 2355.
4. Rasburn, J.; Klein, P. G.; Ward, I. M. J Polym Sci Part B: Polym Phys 1994, 32, 1329.
5. Bonner, M. J.; Duckett, R. A.; Ward, I. M. J Mater Sci 1999, 34, 1885.
6. Sherby, O. D.; Dorn, J. E. J Mech Phys Solids 1956, 6, 165.
7. Ward, I. M.; Wilding, M. A. J Polym Sci Polym Phys Ed 1984, 22, 561.
8. Coates, P. D.; Ward, I. M. J Mater Sci 1978, 13, 629.
9. Coates, P. D.; Gibson, A. G.; Ward, I. M. J Mater Sci 1980, 15, 359.
10. Bonner, M. J. Ph.D. Thesis, University of Leeds, UK, 1994.
11. Wilding, M. A.; Ward, I. M. Polymer 1978, 19, 969.
12. Wilding, M. A.; Ward, I. M. Polymer 1981, 22, 870.
13. Clutton, E. Q.; Rose, L. J.; Capaccio, G. Plast Rubber Compos Appl 1998, 27, 478.
14. Lu, X.; Wang, X.; Brown, N. J Mater Sci 1998, 23, 643.
15. Rose, L. J.; Channell, A. D.; Frye, C. J.; Capaccio, G. J Appl Polym Sci 1994, 54, 2119.